Journal of the Physical Society of Japan
Vol. 79, No. 2, February, 2010, 024005

Generalized Statistical Mechanics and Scaling Behavior for Non-equilibrium Polymer Chains: I. Monomers Connected by Rigid Bonds

Wen-Jong MA[1*] and Chin-Kun HU[1,2†]

[1]*Institute of Physics, Academia Sinica, Nankang, Taipei 11529, Taiwan*
[2]*Center for Nonlinear and Complex Systems, Department of Physics, Chung-Yuan Christian University, Chungli 32023, Taiwan*

(Received July 10, 2009; accepted December 1, 2009; published February 10, 2010)

Using molecular dynamics simulation, we find that the velocity distributions of monomers in the system of non-equilibrium polymer chains and Lennard-Jones molecules in a wide range of simulation time can be well described by Tsallis q-statistics and a single scaling function; the value of q is related to the conformation constraining potential, the interactions with background fluid, or the destruction of chain homogeneity. This approach can be applied to other non-equilibrium systems.

KEYWORDS: scaling, molecular dynamics, polymer, q-statistics
DOI: 10.1143/JPSJ.79.024005

1. Introduction

Scientific research can be considered as a process of data reduction, in the sense that one looks for new ideas and principles so that a variety of phenomena can be understood from some simple universal mechanism, or data from different systems or situations can be represented by one or a few functions with a small number of parameters.[1)] For example, it has been found that critical behaviors of Ising-type spin models[2)] and lattice hard-core particle models[3)] can be understood from percolation transitions of properly defined clusters of the systems as in the case of random percolation models,[4)] that many percolation models[1,5)] or the Ising model[6)] on different lattices have universal finite-size scaling functions,[7)] and that transitions to synchronous chaos of the coupled-map lattice model[8)] with both local and global couplings have good universal and scaling behaviors.[9)]

Using Molecular dynamic (MD) simulation, in the present paper we will show that the velocity distributions of monomers in systems of nonequilibrium polymer chains and Lennard-Jones molecules in a wide range of simulation time can be well described by Tsallis q-statistics[10,11)] and a single scaling function. Our results suggest that complex nonequilibrium systems can still have simple scaling behavior, and inspire further studies in many interesting problems.

The complex spatial and temporal behaviors of non-equilibrium systems have attracted much attention in recent decades. It is of interest to know whether one can extend some ideas of equilibrium statistical mechanics to describe nonequilibrium systems. Recently, Tsallis proposed a generalized statistics, called q-statistics, that has been used to describe many complex systems.[10,11)] Beck and Cohen suggested that such statistics may be interpreted as a universal description of systems characterized by a lack of uniformity in their intensive macroscopic parameters (e.g., the temperature).[12)] While the formulations for such q-statistics are formal and potentially provide a concrete microscopic basis,[13,14)] velocity distributions in various systems seem readily to provide a connection between microscopic theoretical calculations and macroscopic experimental verifications.[15–17)] Since the systems described well by q-statistics often have spatial and temporal complexities, such a verification would require on the theoretical side some detailed information for the nonequilibrium situation. Here we address such issues in molecular dynamics simulations of model systems composed of polymer chains and Lennard-Jones molecules; we find that q-statistics can describe very well the velocity distributions of monomers for nonequilibrium situations in a wide range of simulation time.

Molecular fluctuations in polymers arising from the internal degrees of freedom, mingled with the interactions with environmental particles may affect the thermal and dynamical properties at macroscopic scales.[18,19)] Theoretically, the chain connectivity allows the spatial configuration of a single chain with n monomers, at each instantaneous step, being realized as a constrained random walk, over the chain sequence index i, in three dimensional space. The randomness of such walks explains many material-independent properties in dilute polymer systems,[20,21)] and such randomness in local configurations could render the system to form equilibrium-like meta-stable states. Indeed, one key finding in our simulations is that the steady velocity distributions can be tracked in certain nonequilibrium situations for model polymers mixed in fluids, where the binding between neighboring monomers is realized as strictly rigid. The result may suggest the use of connectivity as a basis for further analysis of dynamics in polymer systems.

2. The Model

In our model, polymer molecules are chains of rigidly connected monomers, interacting via Lennard-Jones potentials between non-bonded monomer pairs and bending and torsion potentials among consecutive sites along the chains. The polymers are modified from the united atom model[22)] where the bond length and the interaction potentials describe polyethylene. The Lennard-Jones potential between non-bonded monomer pairs at sites i and j with the distance r_{ij} is

*E-mail: mwj@mails.phys.sinica.edu.tw
†E-mail: huck@mails.phys.sinica.edu.tw

$$v_{ij}(r_{ij}) = 4\epsilon[(r_{ij}/\sigma)^{-12} - (r_{ij}/\sigma)^{-6}],$$

where σ and ϵ are used as units for length and energy strength, respectively. For bonded pairs, the bond length is set to $b_0 = 0.357\sigma$.

For consecutive sites i, $j = i+1$, $k = i+2$, and $l = i+3$ along a polymer chain, the unit bond vector $\boldsymbol{b}_i$ defines the direction for two consecutive sites indexed by i and $j = i+1$ along the chain and the unit local helicity vector is defined by

$$\boldsymbol{u}_i = \frac{\boldsymbol{b}_i \times \boldsymbol{b}_{i+1}}{|\boldsymbol{b}_i \times \boldsymbol{b}_{i+1}|}.$$

The bending angle and the torsion angles are determined by

$$\cos\theta_{ijk} = \boldsymbol{b}_i \cdot \boldsymbol{b}_j \quad \text{and} \quad \cos\phi_{ijkl} = \boldsymbol{u}_i \cdot \boldsymbol{u}_j,$$

respectively. $180^\circ - \theta_{ijk}$ and ϕ_{ijkl} are, respectively, the valence angle and torsional angle considered in ref. 23. We set the bending potential

$$\Theta(\theta_{ijk}) = K_b 1097\epsilon(\cos\theta_{ijk} - \cos\theta_0)^2, \tag{1}$$

and the torsional potential

$$\Phi(\phi_{ijkl}) = K_t \sum_{\iota=0}^{3} a_i(\cos\phi_{ijkl})^\iota, \tag{2}$$

with $a_0 = 18.635\epsilon$, $a_1 = 38.16\epsilon$, $a_2 = 10.3\epsilon$, and $a_3 = -67.075\epsilon$, as in ref. 22, θ_0 is either $\theta_0^{(\mathrm{I})} = 112.813^\circ$ or $\theta_0^{(\mathrm{II})} = 67.187^\circ$. We consider K_b and K_t, and θ_0 as the tuning parameters related to the polymer properties at longer time and length scales. A cutoff of 2.3σ is used for pair (Lennard-Jones) interactions.

We can express the length σ_F and strength ϵ_F of the Lennard-Jones interactions between fluid molecules in units of σ and ϵ, respectively. All fluid molecules and monomers are assumed to have the same mass m. The composite quantity $\tau = \sqrt{m\sigma^2/\epsilon}$ is used as the time unit. The purely repulsive interaction potential between a monomer and a fluid molecule takes the -12 power term only. Heterogeneous conditions can be introduced into the system by selecting a small portion of monomer sites, imposing different inter-site interactions. By mixing the polymers with spherical Lennard-Jones fluid molecules, the heterogeneous properties can be realized via the varieties of interactions between fluid and polymers. We let the interaction potentials of fluid particles with the ordinary polymer sites be purely repulsive and with the small portions of specially selected sites ("linker sites") on polymers be the same as fluid–fluid potentials. Such a set-up mimics heterogeneities in the hydrophobic–hydrophilic effects in systems of biopolymers and helps to stabilize the system. The shape and the strengths of all those interaction potentials are tunable as the means to alter the physical properties of the simulated system.

In the MD simulations, it is well known that the dynamic properties are related to the detailed numerical implements in solving the equations of motion.[24] In our simplified model, we particularly emphasize the well-tracked formulation of the discretized equations of motion that are treated as iterative dynamic systems. This aspect is appropriate in searching for microscopic origins of q-statistics.[13,14] We numerically solve the equations of motions in Lagrangian formulations, using a velocity Verlet algorithm with the bonding between neighboring monomers realized via the RATTLE scheme[25] to incorporate the holonomic constraints for fixed bond lengths.

3. Simulation Procedure and Results

We choose $K_b = K_t = 0.1$, which are one tenth of those for polyethylene, so that the simulations can cover a longer range of time scales. To start, we fill $N_P = 40$ polymer chains (each chain has $n = 100$ monomers) and $N_F/4 = 1500$ fluid molecules in a large enough cube of volume $V = L^3$ with periodic boundary conditions so that polymer chains can take some arbitrary random initial configurations. We choose θ_0 to be $\theta_0^{(\mathrm{I})} = 112.813^\circ$ in all chains. We select $\sigma_F = \sigma/4$ and let a small N_L (= 199) of randomly selected monomers among the chains interact differently from the majority of the monomers to mimic the hydrophilic-like contacts with fluid particles. We control the pressure and the kinetic energy[26] to adjust the volume V until it reaches some value $V \approx (32.5\sigma)^3$. Then we replace each fluid molecule with four closely packed molecules of zero kinetic energy and allow the new system (of N_P polymers and N_F fluid molecules) to relax and finally reach a volume $V = L^3$ ($L = 33.3875\sigma$).

In molecular dynamic simulations, the external conditions can be controlled dynamically by introducing one or few variables, which can effectively provide statistical ensembles such as NVE, NVT, and NPT for equilibrium systems; here N, V, E, T, and P represent number of particles, volume, energy, temperature, and pressure, respectively.[26] The NPT processes designed for equilibrium simulations have been used in the preparation stage, where we control externally the pressure (P) and the temperature (T) to drive the system to the target density. The process also fine-tunes the conformations of the polymer chains which helps the effective performance of the RATTLE algorithm in the subsequent NVE simulation.

We then start the production simulations with the integration time step $(\delta t)_1 \equiv 5.0 \times 10^{-6}\tau$ and focus on the NVE relaxation processes with constant volume V and total energy E without any external controlling. To speed up the simulation process, we increase the integration time step δt from $(\delta t)_1 \equiv 5.0 \times 10^{-6}\tau$ by five times to $(\delta t)_2 \equiv 2.5 \times 10^{-5}\tau$ at time $t = 13.4\tau$.

The production simulations from $t = 0$ continue for about 180τ (at the final few τ the integration time step is reduced, see below) and the results are shown in Figs. 1 and 2. Figure 1(a) shows that the time evolution of the temperature-like quantities, T_P^*, T_F^* and T_0^*, consist of several stages, where T_P^*, T_F^*, and T_0^* are twice of the mean kinetic energies per degree of freedom for polymer chains, fluid molecules, and the whole system, respectively. For polymer chains, $T_P^* \equiv f^{-1}\sum_{\text{site } i} m_i v_i^2$, where $f = N_P(2n+1)$ is total number of degrees of freedom for polymer chains when $(n-1)$ holonomic constraints for each polymer chain have been taken into account.

In the first stage R_1, the local conformation relaxes with decreasing correlations in bond-pairs [Fig. 1(d)] and local helicity pairs [Fig. 1(e)]. We use inner product $\boldsymbol{b}_i \cdot \boldsymbol{b}_{i+k}$ and $\boldsymbol{u}_i \cdot \boldsymbol{u}_{i+k}$ for indices i and $i+k$ along a chain to define the correlations of index distance k.

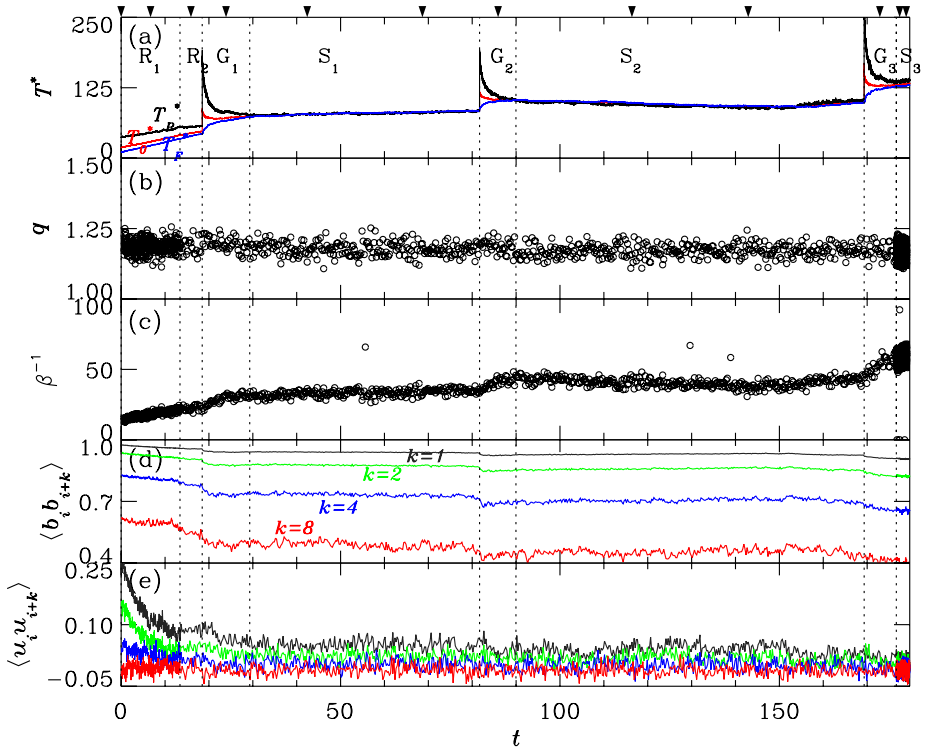

Fig. 1. (Color online) Physical quantities versus time t in the unit of τ. (a) Temperature-like quantities T_0^* (red line), T_P^* (black line), and T_F^* (blue line) in unit ϵ for the whole system, for the polymer sites and for the fluid particles, respectively, in a single step; (b) q; (c) β^{-1}; (d) bond-pair correlation and (e) local helicity-pair correlation, for index distance $k = 1, 2, 4, 8$, in purple, green, blue and red colors, respectively. Data are plotted every 100 steps for (a), and 10000 steps for (b), (c), (d), and (e). The vertical dotted lines mark the change in integration time step δt from $(\delta t)_1 \equiv 5.0 \times 10^{-6}\tau$ to $(\delta t)_2 \equiv 2.5 \times 10^{-5}\tau$ at time $t = 13.4\tau$, dividing the relaxation stage into R_1 and R_2; the intermediate transients, G_1 (from $t = 18.4750$ to 29.2925), G_2 ($t = 81.6725$ to 89.9700), and G_3 ($t = 169.315$ to 176.650) that are followed by the quasi-static stages S_1, S_2, and S_3, respectively. In S_3, the integration step is reduced to $(\delta t)_3 \equiv 5 \times 10^{-7}\tau$. The velocity distributions at those steps marked by inverted triangles on top of plot (a) are analyzed in Fig. 2.

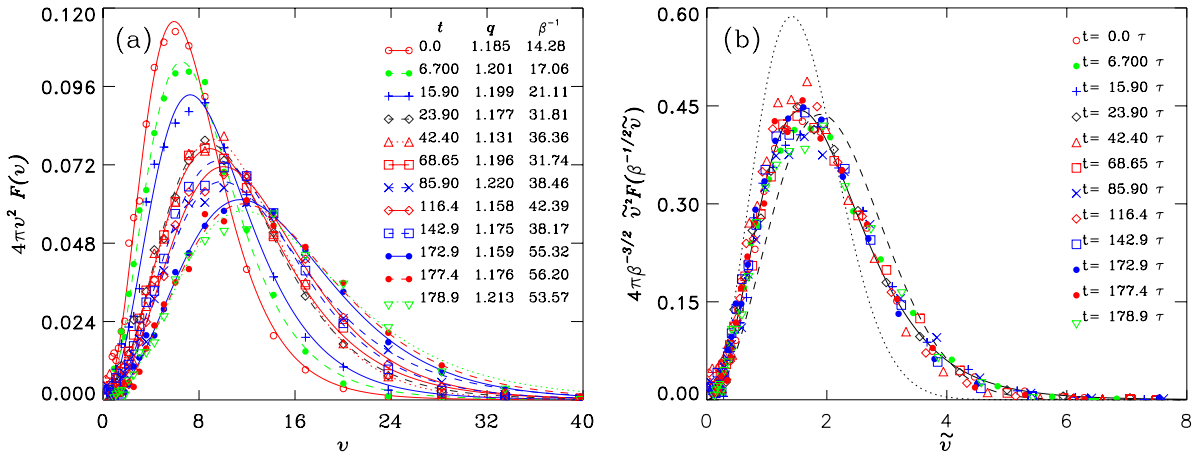

Fig. 2. (Color online) (a) Velocity distributions and (b) scaled velocity distributions, for the system described in Fig. 1. The curves in (a) are the fitted functions [eq. (3)] for the simulated data (in symbols) at the twelve time spots marked in Fig. 1(a). The corresponding time t (in τ) and fitted values q and β^{-1} [Figs. 1(b) and 1(c)] for those curves are listed. The distributions in (b) are rescaled according to eq. (5), where the solid line corresponds to $(q, \beta) = (1.1774, 1.0)$ and the dotted line represents the Maxwell–Boltzmann (MB) distribution with $(q, \beta) = (1.0, 1.0)$. We also plot the MB distribution with $(q, \beta) = (1.0, 0.554)$ as the dashed line, which has the same second moment $\langle \tilde{v}^2 \rangle$ (or $\tilde{T}_P^*$) as that of the solid line.

The increase of the integration time step at $t = 13.4\tau$ would certainly affect the route of time evolution at a microscopic level. Our focus here is on whether the value of q changes. The subsequent relaxation stage R_2 continues before the system becomes quasi-static with $T_P^* \approx T_F^*$. The system is found subject to intermediate transients before and after reaching a quasi-static stage; there are three quasi-static stages, S_1, S_2, and S_3, following the transient stages G_1, G_2, and G_3, respectively. Entering the static stage S_3, we reduce the integration time step by a factor of fifty to $(\delta t)_3 \equiv 5.0 \times 10^{-7}\tau$, to understand its effect on q. From simulation data, we estimated the diffusion constant for monomers as $D \approx 3.3\sigma^2/\tau$. The time spans of S_1 and S_2 are large enough for a monomer to cross a distance ranging from $L/2$ to L.

Figure 2(a) shows that the velocity distributions of monomers at several typical time steps (marked by inverted triangles at the top line of Fig. 1) can be well described by the generalized Maxwell–Boltzmann distribution (GMBD)[15–17]

$$4\pi v^2 F(v) = A_q \beta^{3/2} 4\pi v^2 \times [e_q^{-(\beta/2)mv^2}] \tag{3}$$

where the q-exponential function e_q^x is defined as

$$e_q^x \equiv [1 + (1-q)x]^{1/(1-q)},$$

$$A_q = \left[\int_0^\infty 4\pi v^2 e_q^{-(1/2)mv^2}\, \mathrm{d}v\right]^{-1},$$

and $1 \le q < 7/5$. Note that, in the limit $q \to 1$, eq. (3) becomes the Maxwell–Boltzmann distribution (MBD)

$$4\pi v^2 \left[\left(\frac{m\beta}{2\pi}\right)^{3/2} \times e_q^{-(\beta/2)mv^2}\right]. \tag{4}$$

The parameter β in eq. (3) can be absorbed to scale the velocity variable v,

$$\beta^{-1/2} 4\pi v^2 F(v) = A_q 4\pi \tilde{v}^2 e_q^{-\tilde{v}^2/2}, \tag{5}$$

where $\tilde{v} = \beta^{1/2} v$ and the right-hand-side (RHS) of eq. (5) is free of β, i.e., a family of distributions with different β but the same q can collapse into one master curve.

Figure 2(b) shows that the velocity distributions in Fig. 2(a) collapse into a single curve, after being scaled by using eq. (5). The parameter β^{-1} increases linearly with the instantaneous temperature of monomers T_P^*. The result in Fig. 2(b) suggests that eq. (3) should not be considered merely as a class of fitting functions, it relates the microscopic states over a wide time span as a single non-equilibrium state characterized by the family of distributions of the same q. As for the physical origin of the GMBD, it is useful to consider the ideas of Beck and Cohen.[12]

Note that each distribution in Fig. 2 is over the monomers in the system for one single step. If it is also a probability distribution for an individual monomer, then the x-component of the velocity of particle i satisfies

$$\langle {v_{ix}}^2 \rangle = C_{q,\beta} \int {v_{ix}}^2 e_q^{-\beta K} \prod_{j=1}^{N} \mathrm{d}v_{jx}\, \mathrm{d}v_{jy}\, \mathrm{d}v_{jz}.$$

Using $(e_q^x)' = e_q^x/[1 + (1-q)x]$ and integration by parts, we can derive that the mean kinetic energy of a monomer is

$$\left\langle \frac{1}{2} m v^2 \right\rangle = \frac{3}{2(2-q)} \left[\frac{1}{\beta} - (1-q)\langle K \rangle\right], \tag{6}$$

where K is the total kinetic energy of the polymers. Equation (6) states a modified version of the equipartition theorem; it becomes the conventional equipartition theorem only when $q = 1$. The conditions for the validity of eq. (6), especially the role of heterogeneity,[27] deserve further analysis.

To reveal the determining factors leading to $q > 1$, we carried out simulations manipulating the effect of linker sites or the conformation conditions. Figures 1 and 2 show that the single-step velocity distributions for monomers for different stages in the process are described by GMBD with virtually the same value of q. Reducing the integration time step δt in S_3 in Fig. 1 does not change q. Such an observation is confirmed in Fig. 3, where we include all fitted q collected over the simulations to calculate the (normalized) distribution function $P(q)$. To examine the role played by microscopic non-uniformity, we consider systems with different conditions in fluid-affiliated linker sites or in the conformation constraining (bending and torsion) potentials. We refer to the system described by Figs. 1 and 2 as Case 1. A system in Case 2 has the same interaction and conformation parameters as those of Case 1, except the linker sites are replaced by ordinary monomer sites (homopolymer) and the fluid molecules are removed. For these two systems, a change in the bending angle parameter θ_0 in eq. (1) from $\theta_0^{(\mathrm{I})}$ to $\theta_0^{(\mathrm{II})}$ defines Case 3 and Case 4, respectively. The simulations of the heterogeneous polymer in Case 3 and the two homopolymer systems in Cases 2 and 4 are carried out by starting from the beginning configurations in Fig. 1 and the systems are allowed to relax under NVE conditions. Applying the similar analysis used in Figs. 1 and 2, we collect the data for the distribution $P(q)$ for various stages in Cases 3 (Fig. 3). The distributions for Cases 1 and 3 in Fig. 3 confirm that the same q values are shared by different stages within the same Case. There are, however, obvious differences in the distributions among the comparisons between Case 1 and Case 3. That is, the change in microscopic conformation potentials does affect the value of q. In removing the fluid and the effect of linkers (Case 2 and Case 4), the data suggest a shift toward smaller q. Though such changes are not as large as those caused by the conformation parameter θ_0.

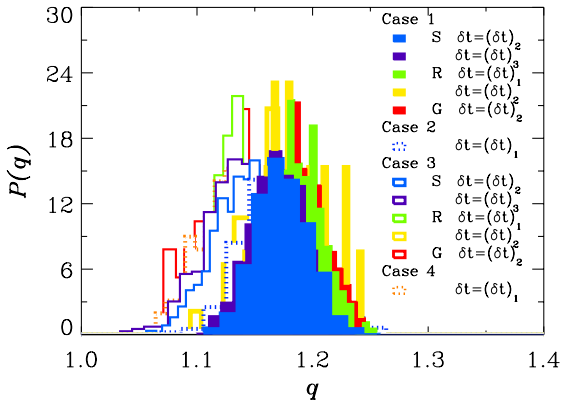

Fig. 3. (Color online) Normalized distribution $P(q)$ of q values for the single-step velocity distributions for various stages in the process of Fig. 1 (Case 1) and Cases 2–4 described in the text. The numbers of collected steps for each stage or case are 522 for S $[(\delta t)_2]$, 608 for S $[(\delta t)_3]$, 266 for R $[(\delta t)_1]$, 21 for R $[(\delta t)_2]$, and 105 for G $[(\delta t)_2)]$ in Case 1; 586 for S $[(\delta t)_2]$, 460 for S $[(\delta t)_3]$, 36 for R $[(\delta t)_1]$, 148 for R $[(\delta t)_2]$, 43 for G $[(\delta t)_2)]$ in Case 3. They are 481 and 301 for Cases 2 and 4, respectively. S represents S_1 or S_2 or S_3, R represents R_1 or R_2, and G represents G_1 or G_2 or G_3.

Our model treats the conformation constraining potentials as the only buffers for the internal motion of polymer chains and, with strict rigid monomer-monomer bonding for polymers, overlooks the varieties in the dynamic modes that may emerge in soft bonding over a range of kinetic energy ($5\epsilon \le T_P^* \le 250\epsilon$ in Case 1). Under such approximation, we have used the smaller (1/10) strengths of the conformation potentials for realistic polymers. Though the information is accurate at coarse-grained levels, the model does provides a concrete example to show that the conformation constraining potentials can result in the anomalies

in velocity distributions. It may lead to some insight into the origin of q-statistics.[10,11,14] Our present and other preliminary studies with various K_b and K_t suggest that the generalized Maxwell–Boltzmann distribution reflects the local dynamics of non equilibrium situations related to the gel or glassy states caused by the conformation constraining potentials. The latter leads to the existence of many metastable states that causes the low relaxation, as in the case of the lattice spin glass at low temperatures.[28] We have found that, for homopolymers with $K_b = K_t \neq 0$, q can still be different from unity for chains as short as $n = 5$. The velocity distributions do return to the ordinary Maxwell–Boltzmann for $n = 2$. The results are consistent with our conjecture that the conformation constraining potentials are responsible for the deviation of q from unity.

4. Discussion

In summary, we have showed that q-statistics can describe velocity distributions of monomers in a non-equilibrium mixture of polymer chains and Lennard-Jones molecules in a wide range of simulation time. Since the switchings among different non-equilibrium stages do not change the value of q, it is worthwhile finding out the relationship between the q-statistics parameters and the content of polymer internal degrees of freedom. Also, a more detailed analysis of the microscopic motion excited over those dynamical transients may provide information about the particular modes of molecular fluctuations, that may be useful in the study of other non-equilibrium systems, such as polymer solutions flowing in nanochannels.[18,19]

In the present paper, neighboring monomers along a polymer chain are connected by rigid bonds. Similar rigid-bond models have been used to represent peptide or protein sequences[29–31] and some reasonably good agreement between the calculated structures of proteins, e.g., HP-36,[30] and those determined in experiments have been obtained from such rigid-bond models. It is of interest to know whether some relaxation and scaling behavior of polymer chains obtained in the present paper can be found in the mixture of biopolymer chains and solvent molecules.

Since neighboring monomers along a polymer chain are connected by rigid bonds, in the present paper, we have used the RATTLE scheme[25] to include the holonomic constraints for fixed bond lengths. To check whether the q-statistics obtained with $q > 1$ are an artifact due to the RATTLE scheme[25] or rigid-bond constraints between neighboring monomers, we use ordinary MD simulations to study the relaxation process in a system of polymer chains and Lennard-Jones molecules, in which each polymer chain consists of monomers connected by springs of strength k_{spring}. The instantaneous temperatures of the monomers in polymer chains, T_P^*, and the fluid, T_F^*, are initially different, but they vary in time and their ratios $\Gamma^* = T_P^*/T_F^*$ approach a constant during the relaxation process. The velocity distributions of monomers in the relaxation process follow q-statistics[10] with $q \geq 1$. We find that the value of q and the limiting ratio of Γ^* depend on k_{spring}; in the strong strength limit, they approach those for the system, in which each polymer chain consists of monomers connected by rigid bonds; in the weak strength limit, Γ^* and q approach 1, corresponding to MB distribution for velocities of monomers. Such results indicate that there is a continuous increase of q as the strength of springs (between monomers) is increased from the smaller to the larger values, and the result $q > 1$ in the present paper is not an artifact of the RATTLE scheme[25] or the rigid-bond constraints.[32]

The aggregation of proteins in human brains can result in neurodegenerative diseases, such as Alzheimer's disease,[33–36] Huntington's disease,[37] Parkinson's disease,[38] etc. Therefore, it is of interest to know relaxation and aggregation behaviors of polymer chains in non-equilibrium situations. The simulation of protein chains with all-atom models of proteins is very time consuming. Therefore, it is better to understand the protein aggregation problem from the simulation of simple polymer chains. We take a system at the end of the simulation of Fig. 1 ($t = 180\tau$) with $q \approx 1.18$ as the initial system and reduce K_b and K_t in eqs. (1) and (2), respectively, to 1.0×10^{-4}. With quenching and heating alternatively, each for about 50τ, we let the system be free from possible residual local structures favored by the original angle potentials. We then let the system be ready to relax. We also consider the case of pure polymers with zero angle potentials ($K_b = K_t = 0$) in the absence of fluid. We find that, in both cases, the turning-down of angle potentials makes the system undergo a slow quenching process, and the polymer chains tend to aggregate. It has been proposed that Alzheimer disease is due to aggregation of proteins Aβ_{40} and Aβ_{42}[34–36] consisting of 40 and 42 residues, respectively. It has been found that Aβ_{40} and Aβ_{42} form β-sheets.[35,36] We may argue that such β-sheets have small or zero effective bending-angle and torsion-angle dependent potentials, and thus they can aggregate as the polymer chains studied by us. Similar arguments might be applied to other proteins which can aggregate. The details of such results will be presented in another paper.

Acknowledgments

We thank S. Abe and Y. L. Chen for useful discussion and Mandy Brannon Engelsma for improving the English presentation. This work was supported by Grants NSC 96-2911-M 001-003-MY3 and AS-95-TP-A07, and NCTS (North) in Taiwan.

1) C.-K. Hu, C.-Y. Lin, and J.-A. Chen: Phys. Rev. Lett. **75** (1995) 193 [Errata; **75** (1995) 2786].
2) A. Coniglio and W. Klein: J. Phys. A **13** (1980) 2775; C.-K. Hu: Phys. Rev. B **29** (1984) 5103; C.-K. Hu: Phys. Rev. B **29** (1984) 5109; C.-K. Hu: Physica A **119** (1983) 609; C.-K. Hu: J. Phys. A **16** (1983) L321.
3) C.-K. Hu and K.-S. Mak: Phys. Rev. B **39** (1989) 2948; C.-K. Hu and K.-S. Mak: Phys. Rev. B **42** (1990) 965; C.-K. Hu and C.-N. Chen: Phys. Rev. B **43** (1991) 6184; G. Giacomin, J. L. Lebowitz, and C. Maes: J. Stat. Phys. **80** (1995) 1379.
4) D. Stauffer and A. Aharony: *Introduction to Percolation Theory* (Taylor and Francis, London, 1992) 2nd ed.; C.-K. Hu: Phys. Rev. B **46** (1992) 6592.
5) C.-K. Hu, C.-Y. Lin, and J.-A. Chen: Physica A **221** (1995) 80; C.-K. Hu and C.-Y. Lin: Phys. Rev. Lett. **77** (1996) 8; C.-K. Hu and F. G. Wang: J. Korean Phys. Soc. **31** (1997) S271; C.-Y. Lin and C.-K. Hu: Phys. Rev. E **58** (1998) 1521; H. P. Hsu, S. C. Lin, and C.-K. Hu: Phys. Rev. E **64** (2001) 016127; H. Watanabe, S. Yukawa, N. Ito, and C.-K. Hu: Phys. Rev. Lett. **93** (2004) 190601; H. Watanabe and C.-K. Hu: Phys. Rev. Lett. **95** (2005) 258902; H. Watanabe and C.-K. Hu: Phys. Rev. E **78** (2008) 041131.
6) Y. Okabe and M. Kikuchi: Int. J. Mod. Phys. C **7** (1996) 287; F. G.

Wang and C.-K. Hu: Phys. Rev. E **56** (1997) 2310; Y. Okabe, K. Kaneda, M. Kikuchi, and C.-K. Hu: Phys. Rev. E **59** (1999) 1585; Y. Tomita, Y. Okabe, and C.-K. Hu: Phys. Rev. E **60** (1999) 2716; M. C. Wu, C.-K. Hu, and N. S. Izmailian: Phys. Rev. E **67** (2003) 065103.
7) V. Privman and M. E. Fisher: Phys. Rev. B **30** (1984) 322.
8) K. Kaneko: Prog. Theor. Phys. **72** (1984) 480; K. Kaneko: Physica D **34** (1989) 1; K. Kaneko: Physica D **41** (1990) 137; P. M. Gade and C.-K. Hu: Phys. Rev. E **60** (1999) 4966; P. M. Gade and C.-K. Hu: Phys. Rev. E **62** (2000) 6409.
9) P. M. Gade and C.-K. Hu: Phys. Rev. E **73** (2006) 036212.
10) C. Tsallis: J. Stat. Phys. **52** (1988) 479.
11) Prog. Theor. Phys. Suppl. **162** (2006).
12) C. Beck and E. G. D. Cohen: Physica A **322** (2003) 267.
13) E. Mayoral and A. Robledo: Phys. Rev. E **72** (2005) 26209; P. Grassberger: Phys. Rev. Lett. **95** (2005) 140601; A. Robledo: Physica A **370** (2006) 449.
14) A. Pluchino, A. Rapisarda, and C. Tsallis: Europhys. Lett. **80** (2007) 26002.
15) J. A. S. Lima and R. Silva: Phys. Lett. A **338** (2005) 272.
16) R. Silva, Jr., A. R. Plastino, and J. A. S. Lima: Phys. Lett. A **249** (1998) 401.
17) P. Douglas, S. Bergamini, and F. Renzoni: Phys. Rev. Lett. **96** (2006) 110601.
18) R. Khare, M. D. Graham, and J. J. de Pablo: Phys. Rev. Lett. **96** (2006) 224505.
19) Y. L. Chen, M. D. Graham, J. J. de Pablo, G. C. Randall, M. Gupta, and P. S. Doyle: Phys. Rev. E **70** (2004) 060901.
20) M. Doi and S. F. Edwards: *The Theory of Polymer Dynamics* (Oxford University Press, New York, 1986).
21) A. Yu. Grosberg and A. R. Khokhlov: *Statistical Physics of Macromolecules* (AIP, New York, 1994).
22) D. Steele: Chem. Soc., Faraday Trans. 2 **81** (1985) 1077.
23) K. Karatasos, A. B. Adolf, and S. Hotston: J. Chem. Phys. **112** (2000) 8695.
24) T. Schlick: *Molecular Modelling and Simulation: An Interdisciplinary Guide* (Springer, New York, 2002).
25) H. C. Andersen: J. Comput. Phys. **52** (1983) 24.
26) M. P. Allen and D. J. Tildesley: *Computer Simulation of Liquids* (Oxford University Press, Oxford, U.K., 1987).
27) C. Vignat and A. Plastino: Phys. Lett. A **343** (2005) 411.
28) C. Dasgupta, S.-K. Ma, and C.-K. Hu: Phys. Rev. B **20** (1979) 3837.
29) U. H. E. Hansmann and Y. Okamoto: J. Comput. Chem. **14** (1993) 1333.
30) C.-Y. Lin, C.-K. Hu, and U. H. E. Hansmann: Proteins **52** (2003) 436.
31) F. Eisenmenger, U. H. E. Hansmann, S. Hayryan, and C.-K. Hu: Comput. Phys. Commun. **138** (2001) 192; F. Eisenmenger, U. H. E. Hansmann, S. Hayryan, and C.-K. Hu: Comput. Phys. Commun. **174** (2006) 422; S. Hayryan, C.-K. Hu, J. Skrivanek, E. Hayryan, and I. Pokorny: J. Comput. Chem. **26** (2005) 334; J. Busa, J. Dzurina, E. Hayryan, S. Hayryan, C.-K. Hu, J. Plavka, I. Pokorny, J. Skrivanek, and M.-C. Wu: Comput. Phys. Commun. **165** (2005) 59; R. G. Ghulghazaryan, S. Hayryan, and C.-K. Hu: J. Comput. Chem. **28** (2007) 715; J. Busa, S. Hayryan, C.-K. Hu, J. Skrivanek, and M. C. Wu: J. Comput. Chem. **30** (2009) 346.
32) W.-J. Ma and C.-K. Hu: J. Phys. Soc. Jpn. **79** (2010) 024006.
33) Heilbronner: Arch. Psychiatr. Nervenkr. **33** (1900) 366.
34) A. Goate, M. C. Chartierharlin, M. Mullan, J. Brown, F. Crawford, L. Fidani, L. Giuffra, A. Haynes, N. Irving, L. James, R. Mant, P. Newton, K. Rooke, P. Roques, C. Talbot, M. Pericakvance, A. Roses, R. Williamson, M. Rossor, M. Owen, and J. Hardy: Nature **349** (1991) 704.
35) A. T. Petkova, Y. Ishii, J. J. Balbach, O. N. Antzutkin, R. D. Leapman, F. Delaglio, and R. Tycko: Proc. Natl. Acad. Sci. U.S.A. **99** (2002) 16742.
36) T. Luhrs, C. Ritter, M. Adrian, D. Riek-Loher, B. Bohrmann, H. Doeli, D. Schubert, and R. Riek: Proc. Natl. Acad. Sci. U.S.A. **102** (2005) 17342.
37) G. Huntington: Med. Surg. Rep. Philadelphia **26** (1872) 317.
38) J. Parkinson: *An Essay on the Shaking Palsy* (Sherwood, Neely, and Jones, London, 1817); M. H. Polymeropoulos, C. Lavedan, E. Leroy, S. E. Ide, A. Dehejia, A. Dutra, B. Pike, H. Root, J. Rubenstein, R. Boyer, E. S. Stenroos, S. Chandrasekharappa, A. Athanassiadou, T. Papapetropoulos, W. G. Johnson, A. M. Lazzarini, R. C. Duvoisin, G. DiIorio, L. I. Golbe, and R. L. Nussbaum: Science **276** (1997) 2045.